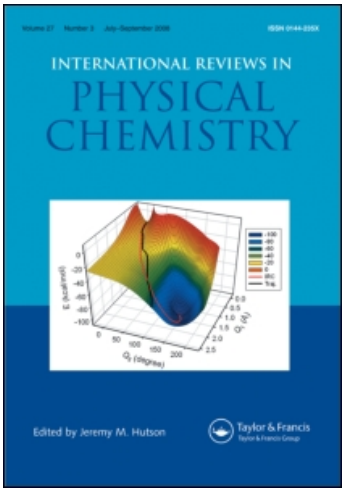

International Reviews in Physical Chemistry
Publication details, including instructions for authors and subscription information:
http://www.informaworld.com/smpp/title~content=t713724383

Grid methods for solving the Schrödinger equation and time dependent quantum dynamics of molecular photofragmentation and reactive scattering processes

Gabriel G. Balint-Kurti[a]; Richard N. Dixon[a]; C. Clay Marston[ab]
[a] School of Chemistry, University of Bristol, Bristol, England [b] Max-Plank-Institüt für Stromungsforschung, Göttingen, Germany

To cite this Article Balint-Kurti, Gabriel G. , Dixon, Richard N. and Marston, C. Clay(1992) 'Grid methods for solving the Schrödinger equation and time dependent quantum dynamics of molecular photofragmentation and reactive scattering processes', International Reviews in Physical Chemistry, 11: 2, 317 — 344
To link to this Article: DOI: 10.1080/01442359209353274
URL: http://dx.doi.org/10.1080/01442359209353274

INTERNATIONAL REVIEWS IN PHYSICAL CHEMISTRY, 1992, VOL. 11, NO. 2, 317–344

Grid methods for solving the Schrödinger equation and time dependent quantum dynamics of molecular photofragmentation and reactive scattering processes

by GABRIEL G. BALINT-KURTI, RICHARD N. DIXON
and C. CLAY MARSTON†
School of Chemistry, University of Bristol,
Bristol BS8 1TS, England

This review will concentrate on new theoretical methods for solving the quantum dynamics of molecular systems. The approach will be that of solving the time dependent Schrödinger equation, and extracting from it the measurable quantities of experimental interest. Applications to the modelling of molecular photodissociation processes and to the theory of reactive molecular collisions will be discussed.

1. Introduction

The time dependent Schrödinger equation may be written in the form:

$$i\hbar\frac{\partial}{\partial t}\psi(x,t)=\hat{\mathscr{H}}\psi(x,t). \tag{1}$$

If the Hamiltonian operator is independent of time, the formal solution of this equation is very simple and may be written in the form:

$$\psi(x,t)=\exp(-i\hat{\mathscr{H}}t/\hbar)\psi(x,t=0), \tag{2}$$

where $\psi(x,t=0)$ represents the initial state of the system.

The right hand side of the above equation contains an 'exponentiated' Hamiltonian operator. Such an exponentiated operator may be evaluated by expanding the exponential in a Taylor series. If this is done the following is obtained:

$$\begin{aligned}\psi(x,t)&=\left[1+(-i\hat{\mathscr{H}}t/\hbar)+(-i\hat{\mathscr{H}}t/\hbar)^2\left(\frac{1}{2!}\right)+(-i\hat{\mathscr{H}}t/\hbar)^3\left(\frac{1}{3!}\right)\ldots\right]\psi(x,t=0)\\&=\left\{1-i[\hat{\mathscr{H}}\psi(x,t=0)]t/\hbar-\{\hat{\mathscr{H}}[\hat{\mathscr{H}}\psi(x,t=0)]\}(t/\hbar)^2\left(\frac{1}{2!}\right)\right.\\&\quad\left.+i\{\hat{\mathscr{H}}\{\hat{\mathscr{H}}[\hat{\mathscr{H}}\psi(x,t=0)]\}\}(t/\hbar)^3\left(\frac{1}{3!}\right)\ldots\right\}.\end{aligned} \tag{3}$$

Equation (3) has been written out in detail so as to show what is required to solve the time dependent Schrödinger equation. The key to solving it lies in our ability to operate on a function (e.g. $\psi(x,t=0)$) with the Hamiltonian operator $\hat{\mathscr{H}}$. We see that all that is needed to solve the equation is repeated operations on $\psi(x,t=0)$ with this operator. In Section 2, where we discuss the basic theory, we will see how the use of Fourier transforms together with that of a grid representation greatly facilitates the evaluation of the necessary expressions.

† Present address: Max-Planck-Institüt für Stromungsforschung, Bunsenstrasse 10, D-3400 Göttingen, Germany.

0144–235X/92 $3·00

The theory of Fourier transforms and the use of grids in coordinate space leads very naturally to a new and extremely transparent method of solving the time independent Schrödinger equation for bound vibrational states of molecules. The theory of this method is presented first of all. At present its main advantage lies on its transparent simplicity, reliability and robustness. As discussed in Section 3 it may eventually transpire that it will form the basis of numerically efficient algorithms for calculating bound molecular vibrational–rotational states.

Section 4 is devoted to discussing the application of time dependent wavepacket computations to the study of photodissociation processes. In particular we describe the procedures we have developed for the analysis of the time dependent wavepacket for the computation of the final fragment quantum state distributions. The method automatically generates the photofragmentation cross-section over the entire photon frequency range of interest from a single dynamical computation. This aspect of time dependent methods constitute one of their main advantages.

In Section 5 we describe the application of the methods to the theory of reactive molecular collisions. The same techniques as have been applied to molecular photofragmentation theory can also be applied here. Some preliminary results are presented and comparisons made with the results of time independent computations. The problems encountered are discussed and new techniques being developed for overcoming them are described. The great advantage of time dependent quantum dynamical techniques is that they can provide information on the reaction cross-section over a large range of collision energies from solving the dynamics of just a single wavepacket motion are again emphasised.

2. Basic theory

2.1. *Coordinate and momentum space and the role of Fourier transforms*

Let us consider a single particle of mass m moving in one linear dimension under the influence of a potential V. The non-relativistic Hamiltonian operator, $\hat{\mathscr{H}}$, may be written as a sum of a kinetic energy and a potential energy operator

$$\hat{\mathscr{H}} = \hat{T} + V(\hat{x}) = \frac{\hat{p}^2}{2m} + V(\hat{x}). \tag{4}$$

We follow here the philosophy of Dirac's book (1958), in that the operators in equation (4) act on vectors of an abstract Hilbert space, and have not yet been cast into any particular representation. The principle representation which we will use is the Schrödinger or coordinate representation, and the Hamiltonian operator $\hat{\mathscr{H}}$, used in equations (1)–(3), was expressed in this representation. The basic vectors or ket's of the coordinate representation are denoted by $|x\rangle$ and are eigenfunctions of the position or coordinate operator $\hat{x}$.

$$\hat{x}|x\rangle = x|x\rangle. \tag{5}$$

The orthogonality and completeness relationships in terms of these basic vectors are

$$\langle x|x'\rangle = \delta(x - x'), \tag{6}$$

$$\hat{I}_x = \int_{-\infty}^{\infty} |x\rangle\langle x| \, dx. \tag{7}$$

The potential is diagonal in the coordinate representation.

$$\langle x'|V(\hat{x})|x\rangle = V(x)\delta(x-x'). \tag{8}$$

The eigenfunctions of the momentum operator are written as

$$\hat{p}|k\rangle = k\hbar|k\rangle. \tag{9}$$

The kinetic energy operator is therefore diagonal in the momentum representation

$$\langle k'|\hat{T}|\hat{k}\rangle = T_k\delta(k-k')$$

$$\equiv \frac{\hbar^2k^2}{2m}\delta(k-k'). \tag{10}$$

We will also require the orthogonality and completeness relationships in terms of the momentum eigenstates;

$$\langle k|k'\rangle = \delta(k-k'), \tag{11}$$

and

$$\hat{I}_k = \int_{-\infty}^{\infty} |k\rangle\langle k|\,\mathrm{d}k, \tag{12}$$

and the transformation matrix elements between the coordinate and momentum representations:

$$\langle k|x\rangle = \frac{1}{(2\pi)^{1/2}}\exp(-\mathrm{i}kx). \tag{13}$$

Equation (4) to (13) are the basic equations needed to derive all the others used in grid methods for solving both the time independent and the time dependent Schrödinger equations. Let us now consider the problem of acting on the wavefunctions, $\psi(x, t=0)$, expressed in coordinate space, with the Hamiltonian operator. The coordinate space wavefunction is really the 'representative' of the state function $|\psi(t=0)\rangle$ in coordinate space, i.e.:

$$\psi(x, t=0) = \langle x|\psi(t=0)\rangle. \tag{14}$$

The action of the Hamiltonian on the wavefunction in the coordinate representation may be written as:

$$\begin{aligned}\hat{\mathscr{H}}\psi(x,t) &= \langle x|\hat{\mathscr{H}}|\psi(t=0)\rangle \\ &= \langle x|[\hat{T}+V(\hat{x})]|\psi(t=0)\rangle \\ &= \langle x|\hat{T}|\psi(t=0)\rangle + \langle x|V(\hat{x})|\psi(t=0)\rangle.\end{aligned} \tag{15}$$

The potential energy operator, $V(\hat{x})$, is local and may be represented (in the coordinate representation) by its values on a grid of points at pre-chosen values of the coordinate x. Its action on the wavefunction therefore involves just the multiplication of the values of V and ψ at each value of x (i.e. x_i) on the grid. The action of the kinetic energy operator is

more complicated. Using the identity operators (equations (7) and (12)) the coordinate representative of $\hat{T}|\psi(t=0)\rangle$ can be written in the form:

$$\begin{aligned}
\langle x|\hat{T}|\psi(t=0)\rangle &= \langle x|\hat{T}\hat{I}_k\hat{I}_x|\psi(t=0)\rangle \\
&= \langle x|\hat{T}\left(\int_{-\infty}^{\infty}|k\rangle\langle k|\,\mathrm{d}k\right)\left(\int_{-\infty}^{\infty}|x'\rangle\langle x'|\mathrm{d}x'\right)|\psi(t=0)\rangle \\
&= \int_{k=-\infty}^{\infty}\int_{x'=-\infty}^{\infty}\langle x|\hat{T}|k\rangle\langle k|x'\rangle\langle x'|\psi(t=0)\rangle\,\mathrm{d}x'\,\mathrm{d}k \\
&= \int_{k=-\infty}^{\infty}\int_{x'=-\infty}^{\infty}\langle x|(\hbar k)^2/2m|k\rangle\langle k|x'\rangle\langle x'|\psi(t=0)\rangle\,\mathrm{d}x'\,\mathrm{d}k \\
&= \frac{\hbar^2}{2m}\frac{1}{2\pi}\int_{k=-\infty}^{\infty}\int_{x'=-\infty}^{\infty}k^2\exp(\mathrm{i}kx)\exp(-\mathrm{i}kx')\psi(x',t=0)\,\mathrm{d}x'\,\mathrm{d}k \\
&= \frac{\hbar^2}{2m}\frac{1}{2\pi}\int_{k=-\infty}^{\infty}\int_{x'=-\infty}^{\infty}k^2\exp(\mathrm{i}k(x-x')]\psi(x',t=0)\,\mathrm{d}x'\,\mathrm{d}k, \qquad (16)
\end{aligned}$$

where we have used equations (4), (9), (13) and (14).

The wavefunction in coordinate space and that in momentum space are related by Fourier transforms:

$$\begin{aligned}
\psi(x,t=0) &= \langle x|\psi(t=0)\rangle \\
&= \langle x|\hat{I}_k\psi(t=0)\rangle \\
&= \langle x|\left(\int_{-\infty}^{\infty}|k\rangle\langle k|\,\mathrm{d}k\right)\psi(t=0)\rangle \\
&= \int_{-\infty}^{\infty}\langle x|k\rangle\langle k|\psi(t=0)\rangle\,\mathrm{d}k \\
\psi(x,t=0) &= \frac{1}{(2\pi)^{1/2}}\int_{-\infty}^{\infty}\exp(\mathrm{i}kx)\,\psi(k,t=0)\,\mathrm{d}k, \qquad (17)
\end{aligned}$$

and similarly:

$$\psi(k,t=0)=\frac{1}{(2\pi)^{1/2}}\int_{-\infty}^{\infty}\exp(-\mathrm{i}kx)\,\psi(x,t=0)\,\mathrm{d}x. \qquad (18)$$

Equation (16) may therefore be rewritten as:

$$\langle x|\hat{T}|\psi(t=0)\rangle=\frac{\hbar^2}{2m}\frac{1}{(2\pi)^{1/2}}\int_{k=-\infty}^{\infty}k^2\exp(\mathrm{i}kx)\,\psi(k,t=0)\,\mathrm{d}k. \qquad (19)$$

In order to operate with the (one dimensional) kinetic energy operator on the wavefunction the following steps are needed:

(1) Fourier transform the wavefunction $\psi(x,t=0)$ to obtain its momentum space representation $\psi(k,t=0)$ (equation (18)).

(2) Multiply by $(\hbar k)^2/2m$ and perform the inverse Fourier transform (equation (19)).

Efficient, grid based, Fourier transform techniques, called fast Fourier transforms (FFT's) have been developed (Press *et al.* 1986) and their use makes this method of computing the action of the kinetic energy operator on the wavefunction very potent. The use of the FFT method in connection with solving the time dependent Schrödinger has been pioneered by Feit *et al.* (1982) and extensively used by Kosloff and Kosloff (1983a, b, 1986, Kosloff 1988). This has opened up an important new area in molecular quantum dynamics (Kulander 1991).

The application of grid methods to the solution of the time independent Schrödinger equation involves the coordinate representation of the Hamiltonian operator. Using equations (8), (10) and (16) we can write this in the form:

$$\begin{aligned}\langle x|\hat{\mathscr{H}}|x'\rangle &= \langle x|\hat{T}|x'\rangle + V(x)\delta(x-x') \\ &= \frac{1}{2\pi}\int_{-\infty}^{\infty} \exp\left[ik(x-x')\right] T_k \,\mathrm{d}k + V(x)\delta(x-x'). \end{aligned} \tag{20}$$

2.2. *Discretization, grids and discrete Fourier transforms*

For any numerical application we need to replace the continuous range of coordinate values x by a grid of N discrete values, x_n. We will use a uniform grid:

$$x_n = n\Delta x, \tag{21}$$

where Δx is the spacing between the grid points. The length of the grid is $L = N\Delta x$. It will be useful first of all to examine the discretization of the normalization integral for a wavefunction $\psi(x)$ (where $\psi(x)$ is the coordinate representative of a state function $\langle x|\psi\rangle = \psi(x)$). The normalization condition for the wavefunction is

$$\int_{-\infty}^{\infty} \psi^*(x)\psi(x)\,\mathrm{d}x = 1. \tag{22}$$

Discretizing this integral on our regular grid of N values of x we obtain:

$$\sum_{n=1}^{N} \psi^*(x_n)\psi(x_n)\Delta x = 1,$$

or

$$\Delta x \sum_{n=1}^{N} |\psi(x_n)|^2 = 1. \tag{23}$$

We may find it convenient in actual computations to define a 'rescaled' wavefunction, ψ_n:

$$\psi_n = (\Delta x)^{1/2}\psi(x_n). \tag{24}$$

The normalization condition in terms of this 'rescaled' wavefunction is:

$$\sum_{n=1}^{N} |\psi_n|^2 = 1. \tag{25}$$

The grid size and spacing chosen in coordinate space determines the reciprocal grid size in momentum space. The total length of the coordinate space covered by the grid is $L = N\Delta x$. This length determines the longest wavelength, and therefore the smallest frequency, which occurs in the reciprocal momentum space.

$$\Delta k = \frac{2\pi}{\lambda_{\max}},$$

$$\Delta k = \frac{2\pi}{L}, \tag{26}$$

where L is the total length of the grid.

This relationship gives us the grid spacing in momentum space. The central point in the momentum space grid is taken as $k=0$, and the grid points are evenly distributed about zero. In analogy to equation (21) the momentum values at the discrete grid points in momentum space are given by

$$k_m = m\Delta k - k_{\min}, \tag{27}$$

where $k_{\min}=(N\pi/L)$. The maximum absolute value of the momentum which can be represented on the grid is therefore $k_{\max}=(N\pi/L)$.

The basic bra's and ket's of our discretized coordinate space give the value of a wavefunction at the grid points.

$$\langle x_n|\psi\rangle = \psi(x_n) = (\Delta x)^{-1/2}\psi_n. \tag{28}$$

The identity operator (equation (7)), which must now be compatible with equations (22), (25) and (28), becomes:

$$\hat{I}_x = \sum_{n=1}^{N} |x_n\rangle \Delta x \langle x_n|. \tag{29}$$

Similarly the orthogonality condition may now be written as:

$$\Delta x \langle x_n|x_l\rangle = \delta_{nl}. \tag{30}$$

The above relationships provide the basis for two important developments. Firstly they enable us to formulate a 'grid' representation of the Hamiltonian operator, which in turn provides us with an exceedingly simple, robust and accurate method for the calculation of bound state wavefunctions (see Section 3 below). Secondly it provides the bridge between the theory of continuous Fourier transforms, which form the basis of most theoretical discussions, and that of discrete Fourier transforms which are necessarily used in all numerical applications. It will be useful for later reference to write down the detailed relationships between the continuous functions, $\psi(x_n)$ and $\psi(k_m)$ (see equations (17) and (18)), evaluated at the grid points in coordinate and momentum space respectively and the discrete values actually used in computations. The relationship between $\psi(x_n)$ and its discretized analogue ψ_n is given in equation (24). From this and the relationships above we find that the representative of the wavefunction in momentum space is:

$$\psi(k_m) = \left(\frac{L}{2\pi}\right)^{1/2}\left[\left(\frac{1}{N}\right)^{1/2}\sum_{n=1}^{N}\exp(-i2\pi nm/N)\psi_n\right]. \tag{31}$$

The term in the square brackets is the discrete Fourier transform of the set of N values ψ_n, and we will denote it by f_m:

$$f_m = \left(\frac{1}{N}\right)^{1/2}\sum_{n=1}^{N}\exp(-i2\pi nm/N)\psi_n, \tag{32}$$

and the relationship between $\psi(k_m)$ and f_m is therefore:

$$\psi(k_m)=\left(\frac{L}{2\pi}\right)^{1/2} f_m. \tag{33}$$

Finally the inverse Fourier transform, giving ψ_n in terms of f_m is (see Press *et al.* 1986):

$$\psi_n=\left(\frac{1}{N}\right)^{1/2} \sum_{n=1}^{N} \exp(i2\pi nm/N) f_m. \tag{34}$$

2.3. *Treatment of angular coordinates using fast Fourier transforms*

The treatment of the angular variables in an analogous manner to that proposed in the preceding two Sections has until now been beset by problems (Kosloff 1988). This arises because the kinetic energy operator in spherical polar coordinates contains awkward inverse powers of $\sin\theta$. In this section we review a solution to this problem proposed recently by one of us (Dixon 1992). Let us consider a three atom system A–BC. If we use a body fixed coordinate system with the BC→A vector being the body fixed Z axis, the overall wavefunction may be written in the form (Balint-Kurti and Shapiro 1979, 1981):

$$\psi=\sum_K C_K^J \left(\frac{2J+1}{8\pi^2}\right)^{1/2} D_{KM}^J(\alpha\beta\gamma)\, R\, r\, \psi(Rr\theta). \tag{35}$$

α, β and γ are the Euler angles describing the overall rotation of the triatomic system. R is the BC–A distance, r is the B–C distance and θ is the angle between these vectors. These internal coordinates are called Jacobi coordinates. If we now take the matrix elements between the $D_{KM}^J(\alpha\beta\gamma)$ functions we obtain the Hamiltonian operator:

$$\hat{\mathscr{H}}=\hat{\mathscr{H}}_{\text{diag}}+\hat{\mathscr{H}}_{\text{non-diag}}, \tag{36}$$

where

$$\hat{\mathscr{H}}_{\text{diag}}=\frac{\hbar^2}{2}\left\{-\frac{1}{\mu}\frac{\partial^2}{\partial R^2}-\frac{1}{\mu'}\frac{\partial^2}{\partial r^2}-\left(\frac{1}{\mu R^2}+\frac{1}{\mu' r^2}\right)\left[\frac{1}{\sin\theta}\frac{\partial}{\partial\theta}\left(\sin\theta\frac{\partial}{\partial\theta}\right)-\frac{K^2}{\sin^2\theta}\right]\right.$$
$$\left.+\frac{1}{\mu R^2}[J(J+1)-2K^2]\right\}+V(Rr\theta). \tag{37}$$

and

$$\langle JM,K\pm1|\hat{\mathscr{H}}_{\text{non-diag}}|JMK\rangle=\frac{\hbar^2}{2\mu R^2}[(J\pm K+1)(J\mp K)]^{1/2}\left[(K\pm1)\frac{\cos\theta}{\sin\theta}\pm\frac{\partial}{\partial\theta}\right]. \tag{38}$$

$\hat{\mathscr{H}}_{\text{non-diag}}$ couples rotational basis functions with the selection rules $\Delta J=\Delta M=0$ and $\Delta K=\pm1$ (Balint-Kurti and Shapiro 1981). The reduced masses in the above equations are given by:

$$\mu=\frac{m_a(m_b+m_c)}{(m_a+m_b+m_c)}, \qquad \mu'=\frac{m_b m_c}{(m_b+m_c)}. \tag{39}$$

We will concern ourselves here mainly with the solution of the angular part of the diagonal Hamiltonian operator (equation (37)). The angular eigenfunctions of this operator are well known to be the associated Legendre functions $P_K^J(\cos\theta)$. A grid method for acting on the wavefunction with the Hamiltonian operator could easily be

developed based on these orthogonal polynomials and the related Gaussian quadrature rules using the discrete variable representation (DVR) methodology advocated by Light and coworkers (Light *et al.* 1985). A major problem with this approach would be that an exact solution would require the coupling of diagonal equations with different K values (K is the helicity or the component of the angular momentum about the body fixed Z axis). The DVR method based on the associated Legendre polynomials would require the use of different grids in the angular variable θ for every one of the different K values occurring, and would present very many complications on this account. The method proposed here uses a regular grid in θ which is independent of the K value.

The angular dependent part of the diagonal kinetic energy operator (equation (37)) is:

$$\hat{\mathscr{H}}_{\text{diag}} = -\frac{\hbar^2}{2}\left(\frac{1}{\mu R^2}+\frac{1}{\mu' r^2}\right)\left[\frac{1}{\sin\theta}\frac{\partial}{\partial\theta}\left(\sin\theta\frac{\partial}{\partial\theta}\right)-\frac{K^2}{\sin^2\theta}\right]. \tag{40}$$

The centrifugal potential proportional to $(K^2/\sin^2\theta)$ imposes a boundary condition that $\psi(Rr\theta)$ varies with θ as θ^K at small θ and $(\pi-\theta)^K$ as $\theta\to\pi$ (cf. the associated Legendre polynomials). To satisfy this condition ψ is represented as the product:

$$\psi(Rr\theta) = (\sin\theta)^m \phi(Rr\theta), \tag{41}$$

where we choose $m=0$ for K even and $m=1$ for K odd.

The wavefunction ϕ is then represented as a linear combination of the functions $\cos(n\theta)$, and because of this we can use the theory of discrete cosine transforms in the formalism. In order to avoid the singularities in the operator at $\theta=0$ and at $\theta=\pi$ we use a half integral regular mesh of points between $\theta=0$ and π. The relevant discrete quarter-wave Fourier transforms are:

$$F(n) = \sum_{l=1}^{N} 4\phi(\theta_l)\cos(n\theta_l), \qquad 0\leqslant n\leqslant N-1, \tag{42}$$

and the reverse Fourier transform is given by:

$$\phi(\theta_l) = \sum_{n=0}^{N-1}\frac{(2-\delta_{n,0})}{4N}F(n)\cos(n\theta_l). \tag{43}$$

where the grid points have been chosen to be:

$$\theta_l = (2l-1)\pi/2N, \qquad 1\leqslant l\leqslant N. \tag{44}$$

Using a recursion relationship between the products of cosines we can show that:

$$\begin{aligned}\left[\frac{1}{\sin\theta}\frac{\partial}{\partial\theta}\left(\sin\theta\frac{\partial}{\partial\theta}\right)-\frac{K^2}{\sin^2\theta}\right](\sin\theta)^m\cos(n\theta)&\\ = -(\sin\theta)^m\left\{\left[\frac{(K^2-m^2)}{\sin^2\theta}+(n+m)(n+m+1)\right]\cos(n\theta)\right.&\\ \left.+n(2m+1)\sum_{j=\frac{1}{2}(n \bmod 2)}^{\frac{1}{2}(n-2)}(2-\delta_{j,0})\cos(2j\theta)\right\},&\end{aligned} \tag{45}$$

In this equation j is integral for n even, half-integral for n odd, and increases in steps of 1. Thus $2j$ is only even for n even, and odd for n odd. The action of the angular part of

the Hamiltonian (equation (40)) on the angular wavefunction may therefore be written in the form:

$$\begin{aligned}
\mathscr{H}_{\text{diag}}\psi(\theta) &= -\frac{\hbar^2}{2}\left(\frac{1}{\mu R^2}+\frac{1}{\mu' r^2}\right)\left[\frac{1}{\sin\theta}\frac{\partial}{\partial\theta}\left(\sin\theta\frac{\partial}{\partial\theta}\right)-\frac{K^2}{\sin^2\theta}\right]\psi(\theta) \\
&= \frac{\hbar^2}{2}\left(\frac{1}{\mu R^2}+\frac{1}{\mu' r^2}\right)\left\{\frac{K^2}{\sin^2\theta}\psi(\theta)\right. \\
&\quad \left.-\sum_{n=0}^{N-1}\frac{(2-\delta_{n,0})}{4N}F(n)\left[\frac{1}{\sin\theta}\frac{\partial}{\partial\theta}\left(\sin\theta\frac{\partial}{\partial\theta}\right)\right](\sin\theta)^m\cos(n\theta)\right\} \\
&= \frac{\hbar^2}{2}\left(\frac{1}{\mu R^2}+\frac{1}{\mu' r^2}\right)\left\{\frac{(K^2-m^2)}{\sin^2\theta}\psi(\theta)\right. \\
&\quad +\sum_{n=0}^{N-1}\frac{(2-\delta_{n,0})}{4N}F(n)(\sin\theta)^m\left[(n+1)(n+m+1)\cos(n\theta)\right. \\
&\quad \left.\left.+n(2m+1)\sum_{j=\frac{1}{2}(n \bmod 2)}^{\frac{1}{2}(n-2)}(2-\delta_{j,0})\cos(2j\theta)\right]\right\} \\
&= \frac{\hbar^2}{2}\left(\frac{1}{\mu R^2}+\frac{1}{\mu' r^2}\right)(\sin\theta)^m\left\{\frac{(K^2-m^2)}{\sin^2\theta}\phi(\theta)\right. \\
&\quad +\sum_{n=0}^{N-1}\frac{(2-\delta_{n,0})}{4N}\left[(n+m)(n+m+1)F(n)\right. \\
&\quad \left.\left.+\sum_{j=\frac{1}{2}n}^{\frac{1}{2}(N-1)}2j(2m+1)(2-\delta_{n,0})F(2j)\right]\cos(n\theta)\right\}. \\
&\equiv \frac{\hbar^2}{2}\left(\frac{1}{\mu R^2}+\frac{1}{\mu' r^2}\right)(\sin\theta)^m\left[\frac{(K^2-m^2)}{\sin^2\theta}\phi(\theta)\right. \\
&\quad \left.+\sum_{n=0}^{N-1}\frac{(2-\delta_{n,0})}{4N}G(n)\cos(n\theta)\right], \qquad (46)
\end{aligned}$$

where

$$\begin{aligned}
G(n) &= \left[(n+m)(n+m+1)F(n)+(2m+1)\right. \\
&\quad \left.\times\sum_{j=(n+2)/2}^{\frac{1}{2}(N-1)}2j(2-\delta_{n,0})F(2j)\right], \qquad 0\leqslant n\leqslant(N-3) \\
&= (n+1)(n+m+1)F(n), \qquad (N-2)\leqslant n\leqslant(N-1). \qquad (47)
\end{aligned}$$

Equations (46) and (47) show in detail how the operation on an angular wavefunction of the angular part of the Hamiltonian operator may be performed using an FFT type technique. The operation contains two parts. The first term involves the multiplication of the angular wavefunction $\phi(\theta)$ by a centrifugal potential. The first step for the second term is to perform the discrete FFT of the angular wavefunction ϕ (equation (42)) and so obtain the Fourier amplitudes $F(n)$ in the 'momentum' space conjugate to the angular space. The vector of numbers $G(n)$ (equation (47)) is then constructed by very simple combinations of integers and the $F(n)$ Fourier transform

coefficients. Finally the $G(n)$ are subjected to an inverse Fourier transform and multiplied by the inertial factor. Note that the premultiplier $(\sin\theta)^m$ factors out of the equation, and need not be carried through during the propagation of $\phi(Rr\theta)$.

3. Bound states and the solution of the time independent Schrödinger equation: The Fourier grid Hamiltonian method (FGH)

Equation (20) provides a convenient representation of the Hamiltonian operator in coordinate space. If we replace the basic vectors $|x\rangle$ associated with the continuous space by the discretized analogues, $|x_n\rangle$ we immediately obtain a grid representation of the Hamiltonian operator. This discretized representation provides a Hamiltonian matrix whose dimensions are those of the number of grid points. The matrix elements of this matrix are trivially simple to compute. Indeed we present below a new analytic expression for these matrix elements. The potential, evaluated at the relevant grid points, appear only on the diagonal elements of the matrix. No integrations over a set of basis functions are required to compute the potential energy matrix elements as is normally the case in variational calculations of bound state wavefunctions. It has been shown (Marston and Balint-Kurti 1989, Balint-Kurti *et al.* 1991) that if the values of the wavefunction at the grid points are regarded as the variational parameters, and these are varied to minimize the energy, we arrive at the conclusion that the eigenvalues of the Hamiltonian matrix just mentioned are the bound state energies of the nuclear motion of the system (rotational–vibrational energy levels) and the corresponding eigenvectors give the value of the wavefunction at the grid points.

Directly from the coordinate representation of the Hamiltonina operator (equation (20)) we obtain:

$$\begin{aligned} H_{ij} &= \langle x_i|\hat{\mathscr{H}}|x_j\rangle \\ &= \frac{1}{2\pi}\sum_{l=-(n-1)}^{n} \exp\left[il\Delta k(x_i-x_j)\right]\left[\frac{\hbar^2}{2m}(l\Delta k)^2\right]\Delta k + \frac{V(x_i)\delta_{ij}}{\Delta x} \\ &= \frac{1}{\Delta x}\left\{\sum_{l=-(n-1)}^{n} \frac{\exp\left[il2\pi(i-j)/N\right]}{N}\left[\frac{\hbar^2}{2m}(l\Delta k)^2\right] + V(x_i)\delta_{ij}\right\}, \end{aligned} \tag{48}$$

where

$$\Delta k = \frac{2\pi}{N\Delta x}. \tag{49}$$

N is the (even) number of grid points and $n = N/2$. We now define a renormalized Hamiltonian matrix:

$$H^0_{ij} = \Delta x H_{ij}. \tag{50}$$

which is just the term in curly brackets in equation (48).

$$H^0_{ij} = \frac{1}{N}\left\{\left\{\sum_{l=1}^{(n-1)} 2\cos\left[l2\pi(i-j)/N\right]T_l\right\} + (-1)^{(i-j)}T_{N/2}\right\} + V(x_i)\delta_{ij}, \tag{51}$$

where

$$T_l = \frac{\hbar^2}{2m}(l\Delta k)^2 = \frac{1}{2m}\left(\frac{lh}{L}\right)^2.$$

The summation in equation (51) may be performed analytically (Gradshteyn and Ryzhik 1965, Colbert and Miller 1992) to yield:

$$H_{ij}^0 = \frac{h^2}{4mL^2}\left[\frac{(N-1)(N-2)}{6}+1\right]+V(x_i)\delta_{ij}, \qquad \text{if } i=j,$$

$$= \frac{(-1)^{(i-j)}}{m}\left\{\frac{h}{2L\sin[\pi(i-j)/N]}\right\}^2, \qquad \text{if } i\neq j. \tag{52}$$

Figure 1 shows a Morse potential energy curve with parameters corresponding to an HF molecule and also the definition of the evenly spaced grid. Figure 2 shows the tenth bound state wavefunction obtained by diagonalizing the Hamiltonian matrix above using the potential function of figure 1. The methods described above have been used in both one (Chu 1990) and two-dimensional (Lehr and Chatzidimitriou-Dreismann 1991) computations of quasi-bound resonance states and their use for multi-dimensional bound state calculations is being investigated.

4. Molecular photofragmentation theory

The use of time dependent quantum dynamics in the discussion of photodissociation processes was pioneered by Heller and coworkers (Heller 1978, 1979, Kulander and Heller 1978, Lee and Heller 1979). Their implementation of the theory generally made use of approximate semiclassical methods of solving for the time dependent motion of the wavepacket. The work of Kosloff (Kosloff and Kosloff (1983, 1986), Kosloff, Leforestier *et al.* (1991): see also Heather and Metiu (1987)) showed how the quantum theory could be solved exactly in a practical manner. Since that time there have been many papers applying these methods to the calculation of photodissociation line shapes (Gray and Wozny 1991, Tang *et al.* 1991, Untch *et al.* 1991a, b), Williams *et al.* 1991, Zhang *et al.* 1991). The product quantum state distributions are also of interest, and we review below our own method for computing these quantities. Another interesting quantity which may be computed using time dependent quantum dynamics is the emission spectrum of the molecule during its breakup process. All these aspects of the theory are illustrated through the discussion of the photodissociation of H_2S in its first absorption band.

Contrary to many previously held views of photodissociation processes in small molecules these processes often, or even normally, involve several electronically excited states of the molecule (Dixon 1985). Figure 3 shows, in schematic form, the potential energy curves arising from the modelling of the photodissociation of H_2S (Dixon *et al.* 1990, Schinke *et al.* 1991). It was found that the spectral line shape of the first u.v. absorption band of H_2S could not be modelled using only a single excited electronic state, and required the use of two electronic states as shown in the figure (figure 3). The experimental and theoretically computed absorption line shapes are shown in figure 4. The distinguishing feature of this spectrum is that at low frequencies there is very little structure, and a regular structure sets in at about 50 000 cm^{-1}. This agrees qualitatively with the situation depicted in figure 3. The regular structure arises from the bound states associated with the potential marked V_{22}. It has a sharp onset because it only starts at the energy corresponding to the lowest bound state of this potential.

The photodissociation process starts with the molecule in a bound vibrational–rotational state of its ground electronic state. Let us denote this wavefunction by $\psi_i(R, r, E_i)$. The molecule absorbs a quantum of light and is excited to a higher

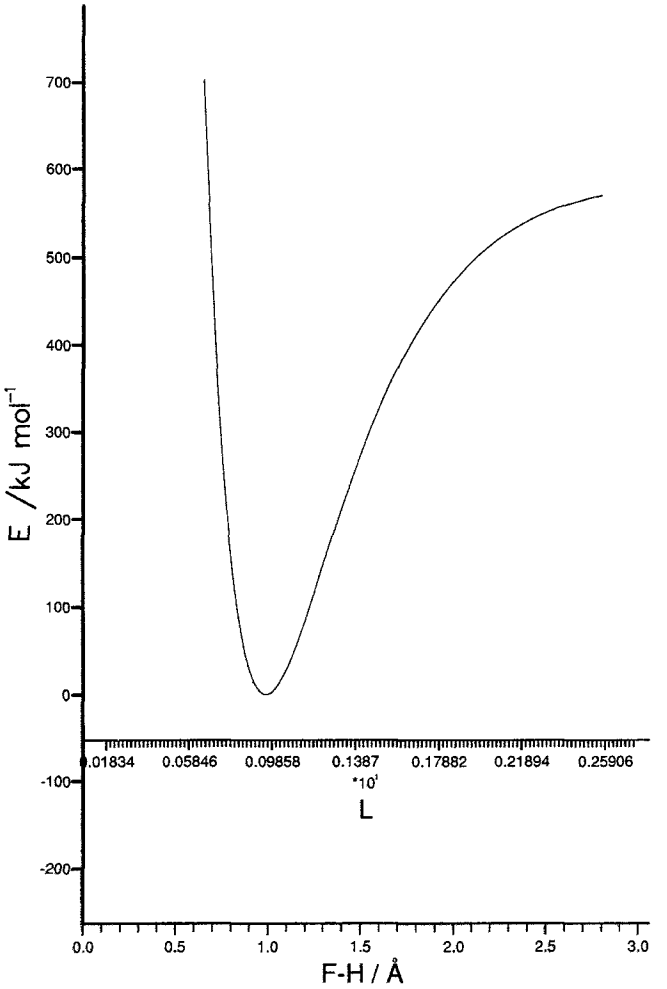

Figure 1. Morse potential energy curve for HF molecule showing definition of one-dimensional grid.

electronic state. It has been shown (Heller 1978, Krishna and Coalson 1988, Balint-Kurti *et al.* 1990) that the spectroscopic absorption cross-section may be obtained by the following computational procedure.

(1) Create the initial wavepacket $\Phi(R,r,t=0)=\mu(R,r)|\psi_i(R,r,E_i)\rangle$, where $\mu(R,r)$ is the transition dipole moment associated with the spectroscopic transition. (Note that we use only two coordinates in the discussion).

(2) Propagate the wavefunction forward in time by using the grid techniques outlined above (equation (19)) and the methods described in the work of Kosloff (1988) to obtain the time dependent wavepacket $\Phi(R,r,t)$ at a series of closely spaced time steps.

(3) At each time step compute the autocorrelation function $F(t)$:

$$F(t)=\langle\Phi(R,r,t=0)|\Phi(R,r,t)\rangle. \tag{53}$$

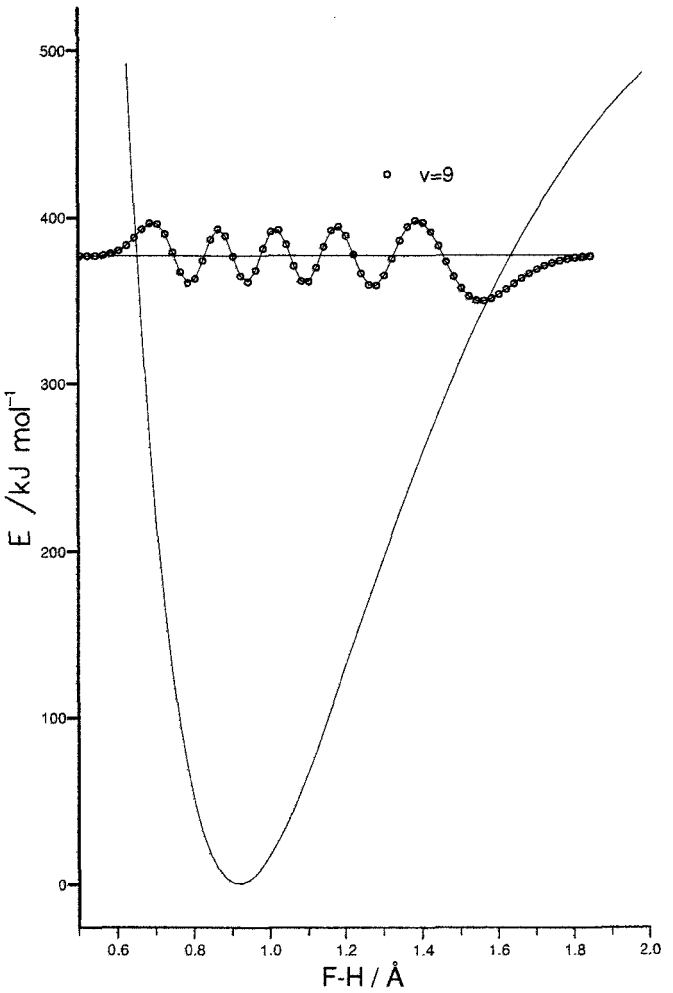

Figure 2. Vibrational wavefunctions for $v=9$ vibrational state of HF molecule computed using the Fourier grid Hamiltonian method.

(4) The total absorption cross-section is then given by the Fourier transform over time of this autocorrelation function:

$$\sigma_i^{\mathrm{Tot}}(v)=\frac{\pi v}{3c\epsilon_0\hbar}2\,\mathrm{Re}\left\{\int_{t=0}^{\infty}\exp(\mathrm{i}Et/\hbar)\,F(t)\,\mathrm{d}t\right\}$$

$$=\frac{\pi v}{3c\epsilon_0\hbar}2\,\mathrm{Re}\left\{\int_{t=0}^{\infty}\exp(\mathrm{i}Et/\hbar)\,\langle\Phi(R,r,t=0)|\Phi(R,r,t)\rangle\,\mathrm{d}t,\right\} \qquad (54)$$

where $E=E_i+hv$.

Using this approach the spectral absorption line shape is obtained over all photon energies from a single computation of the molecular dynamics.

Figure 5 shows the dissociative electronically excited potential energy surface (V_{11} of figure 3) which emerged from the modelling of the $H_2S+hv\rightarrow HS(v)+H$ photodissociation process in its first u.v. absorption band, while figure 6 shows several

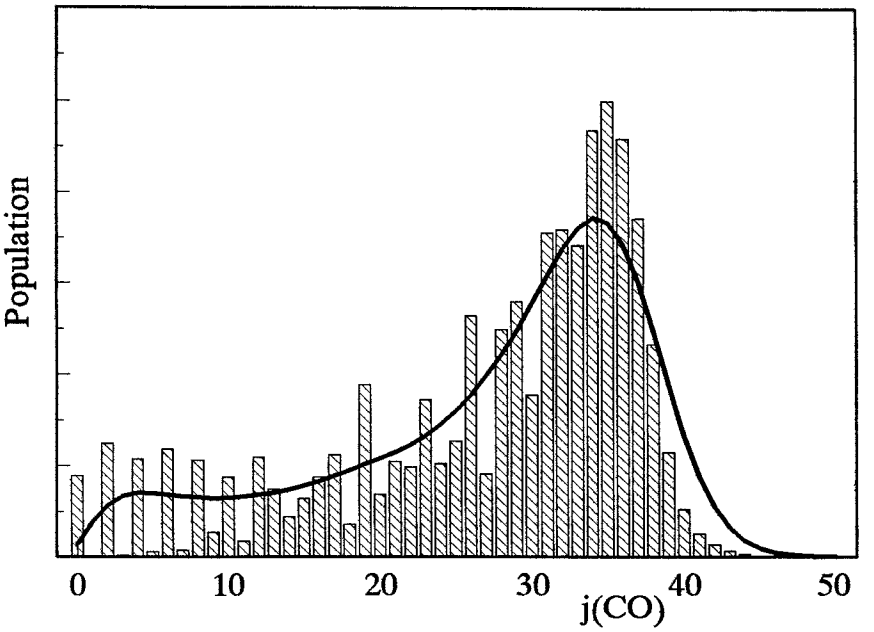

Figure 10. The rotational distribution of the CO fragment calculated for excitation of HCO to an energy of 17 750 cm^{-1}, in simulation of the predissociation of levels of the $\tilde{A}$ state. Histogram: calculation for $J(HCO)=0$. Curve: simulation for a thermal HCO sample at 70 K.

1990). The figure shows the rotational product quantum state distribution for a single energy. The analysis however generates a (discretized) continuum of such diagrams—a product quantum state distribution for every energy obtained from the time to energy Fourier transform (equation (57)).

On physical ground it is clear that it should be possible to compute any quantity of experimental interest from a knowledge of the time evolution of the wavepacket $(\Phi(R,r,t)=\exp(-i\hat{\mathscr{H}}t/\hbar)\mu(R,r)|\varphi_i(R,r,E_i)\rangle)$. One other such quantity which is currently of great interest is the emission spectrum of a molecule during its decomposition, the decomposition itself having been caused by the absorption of a photon of light. There are therefore two radiation frequencies involved, that of the incident radiation which causes the photodissociation (ν_I) and that of the emitted radiation (ν_S). The cross-section for the emission of radiation of frequency ν_S is given by:

$$\sigma^R(\nu_I,\nu_S)=\frac{\pi^2\nu_I\nu_S^3}{\epsilon_0^2c^4\hbar^2}|f(\nu_I)|^2, \tag{59}$$

where

$$f(\nu_I)=\int_{t=0}^{\infty}\exp[i(E_i+h\nu_I)t/\hbar]\langle\chi_f(R,r,E_f)|\Phi(R,r,t)\rangle\,dt. \tag{60}$$

After the emission of the radiation the molecule is in the vibrational state with wavefunction $\chi_f(R,r,E_f)$ and energy $E_f=E_i+h(\nu_I-\nu_S)$. Figure 11 shows some model bound state vibrational wavefunctions computed for H_2S using a local mode approximation which we have found to fit the stretching energy levels quite accurately (see Dixon *et al.* (1990)). The approximation ignores the bending coordinate and treats

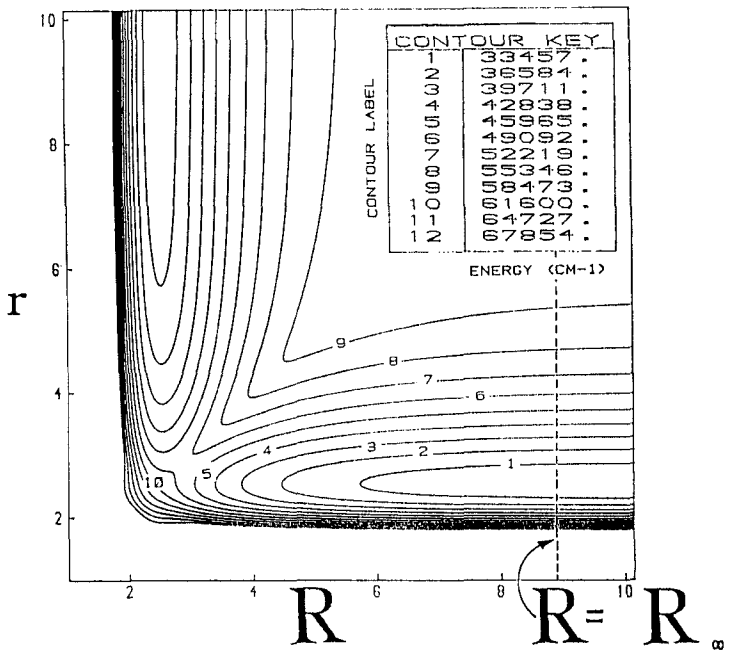

Figure 5. Dissociative excited electronic state potential energy surface modelled to fit the $H_2S+h\nu \rightarrow HS+H$ photodissociation process in its first u.v. absorption band. The line marked $R=R_\infty$ is the 'analysis' line discussed in the text.

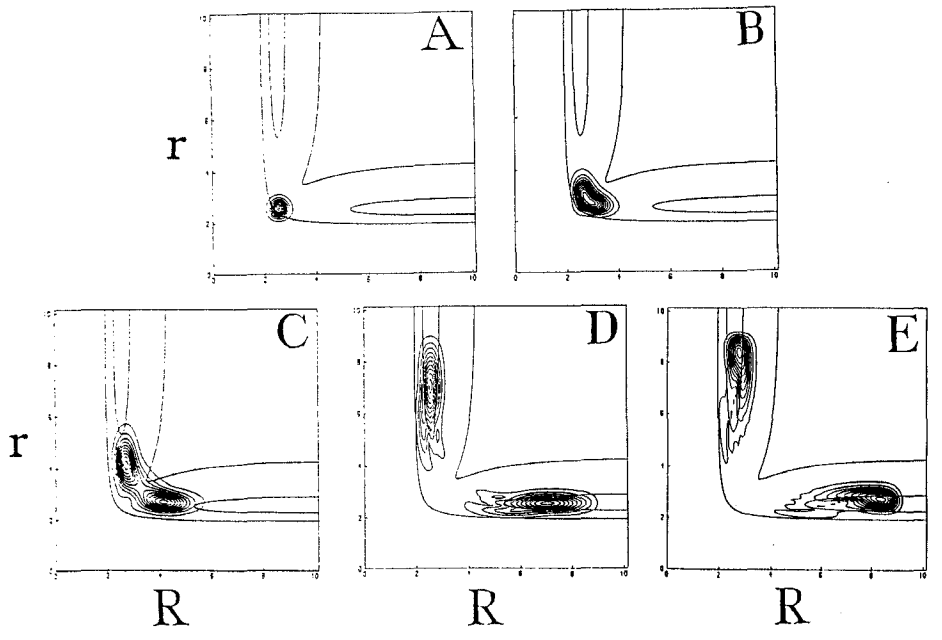

Figure 6. Time dependent motion of the wavepacket representing the photodissociation of H_2S on its first dissociative excited electronic potential energy surface. Snapshots of the wavepacket are shown at time intervals of $\Delta t = 4$ fs. The absolute value of the wavefunction is plotted. (Frames C and D are separated by 8 fs).

'snapshots' of the time development of the wavepacket on this surface. In figure 5 a line marked $R=R_\infty$ is shown, which we call the 'analysis' line. By examining the wavepacket along this 'cut' at every time step it is possible to compute the 'partial' cross-sections which measure the probability of the process producing a particular final fragment quantum state (Balint-Kurti *et al.* 1990). Denoting the HS diatomic vibrational wavefunctions by $\phi_v(r)$, the time evolving wavepacket is analysed at each time step by taking a cut through it at a fixed R value (or HS–H distance) corresponding to $R=R_\infty$ and expanding it in terms of the asymptotic fragment wavefunctions $\phi_v(r)$:

$$\Phi(R=R_\infty, r, t)=\sum_v C_v(R_\infty, t)\phi_v(r), \tag{55}$$

where

$$\begin{aligned} C_v(R_\infty, t)&=\int_0^\infty \phi_v^*(r)\Phi(R=R_\infty, r, t)\,\mathrm{d}r \\ &=\langle\phi_v(r)|\Phi(R=R_\infty, r, t)\rangle. \end{aligned} \tag{56}$$

These time dependent expansion coefficients are now Fourier transformed to give an energy dependent amplitude:

$$\begin{aligned} A_v(R_\infty, E)&=\frac{1}{2\pi}\int_{t=0}^\infty \exp(\mathrm{i}Et/\hbar)\,C_v(R_\infty, t)\,\mathrm{d}t \\ &=\frac{1}{2\pi}\int_{t=0}^\infty \exp(\mathrm{i}E/\hbar)\,\langle\phi_v(r)|\Phi(R_\infty, r, t)\rangle\,\mathrm{d}t. \end{aligned} \tag{57}$$

The squares of the energy dependent amplitudes, $A_v(R_\infty, E)$, are then proportional to the sought-after partial cross-sections†:

$$\sigma_{i\to v}(v)=\frac{4\pi^3 v k_v}{3c\epsilon_0\mu}|A_v(R_\infty, E)|^2. \tag{58}$$

The time dependent coefficients $C_v(R_\infty, t)$ (equation (56)) for the photodissociation of H_2S are shown in figure 7 for the various vibrational quantum states of the HS(v) fragment. The partial cross-sections for the production of each individual fragment vibrational quantum state are obtained by taking the Fourier transforms of these coefficients (equation (57)) and then squaring the resulting energy dependent coefficients (equation (58)). Figure 8 shows the partial cross-sections obtained in this way. The coefficients $C_v(R_\infty, t)$ (figure 7) for vibrational states $v=0, 1$ and 2 show some subsidiary structure after the main smooth hump. Such structure is similar to that which sometimes occurs in the autocorrelation function. As in that case it gives rise an oscillatory contribution to the corresponding partial cross-section versus energy plots (figure 8) which are otherwise smooth. The origin of such oscillations has been previously discussed in several publications (Heller 1981, Balint-Kurti *et al.* 1990). The forms of the predicted partial cross-sections for each vibrational state may be compared with the experimental measurements of Xie *et al.* (1990) and are found to

† Note that this equation differs by a factor of $16\pi^2$ from that given in Balint-Kurti *et al.* 1990). This difference arises from the omission of a factor of 4π in the equation for the energy normalized continuum wavefunction.

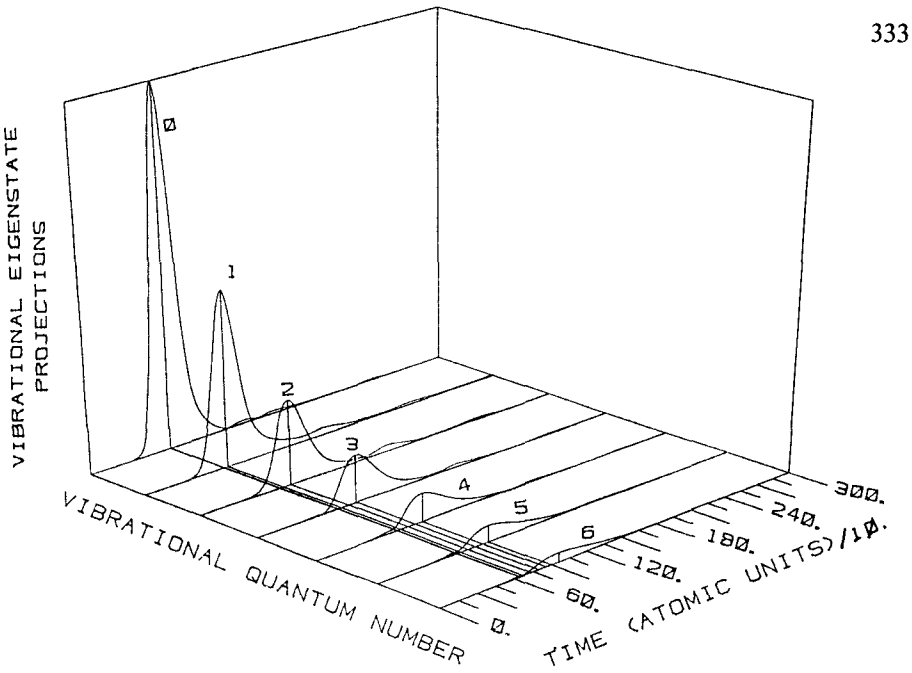

Figure 7. Absolute values of the time dependent expansion coefficients (equation (55)) from vibrational analysis of the wavepacket along the analysis cut in the exit channel (i.e. $R = R_\infty$, see figure 5). The vibrational quantum numbers correspond to the asymptotic photofragment HS states (reproduced with permission from *J. chem. Phys.*, 1990, **93,** 6520).

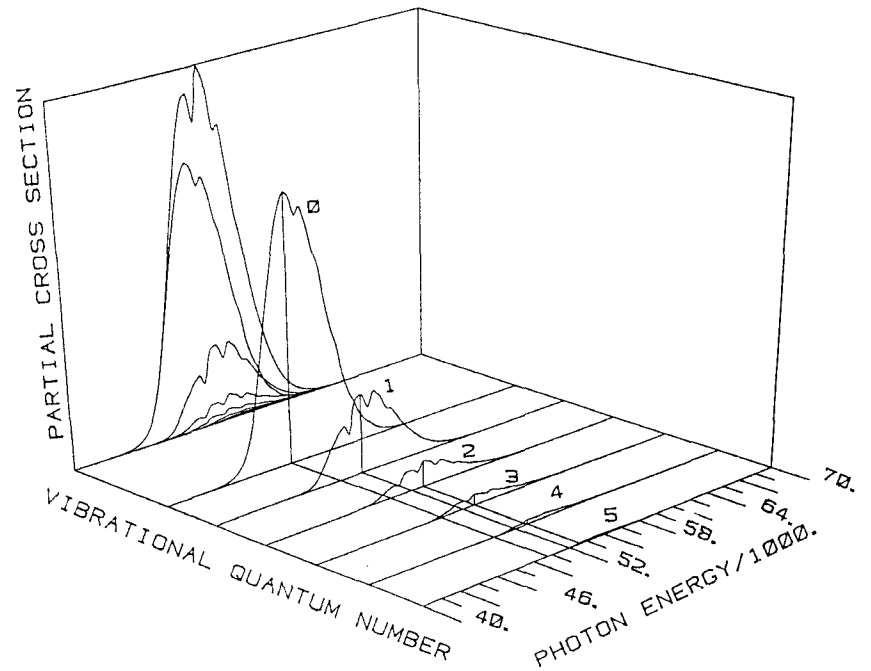

Figure 8. Calculated partial cross-sections (equation (57)) for the production of individual HS photofragment vibrational quantum states as a function of photon energy. The sum of the partial cross-sections are shown on the back plane (reproduced with permission from *J. chem. Phys.*, 1990, **93,** 6520).

agree well for the first few vibrational states ($v=0, 1$ and 2) but to be too great in magnitude for higher vibrational states, showing need for an improved model of the photodissociation process. As in the case of the calculation of the absorption spectrum from the autocorrelation function (equation (54) and figure 4) we see that a single computation of the wavepacket dynamics provides all of the partial cross-sections for the production of each of the photofragment quantum states over the entire energy range of interest.

The same method of analysing the product quantum state population may be used for the determination of the population distribution of the rotational states of dissociation fragments. Figure 9 shows a wavepacket for the dissociation of H–CO on its ground electronic state potential energy surface (Dixon 1992). The horizontal axis of the figure corresponds to the H–CO dissociation coordinate, while the vertical axis is the Jacobi angle between the H–CO vector and the C–O diatomic axis. The initial wavepacket was prepared so as to correspond to one which might result from a curve crossing near linearity from an electronically excited potential energy surface to the ground state surface. This initial wavepacket is shown centred around $\Theta=0°$, $R=1{\cdot}9$ Å. The dissociating wavepacket is shown at a later time in the region of 40°–100°. The analysis line ($R=R_\infty$) is also shown on the diagram and corresponds exactly to that shown in figure 5. The partial cross-sections for the production of different rotationally excited states are obtained by an analysis identical to that outlined for vibrational product quantum states in equations (55–58). Figure 10 shows the results of this analysis, which is in agreement with available experimental results (Kable *et al.*

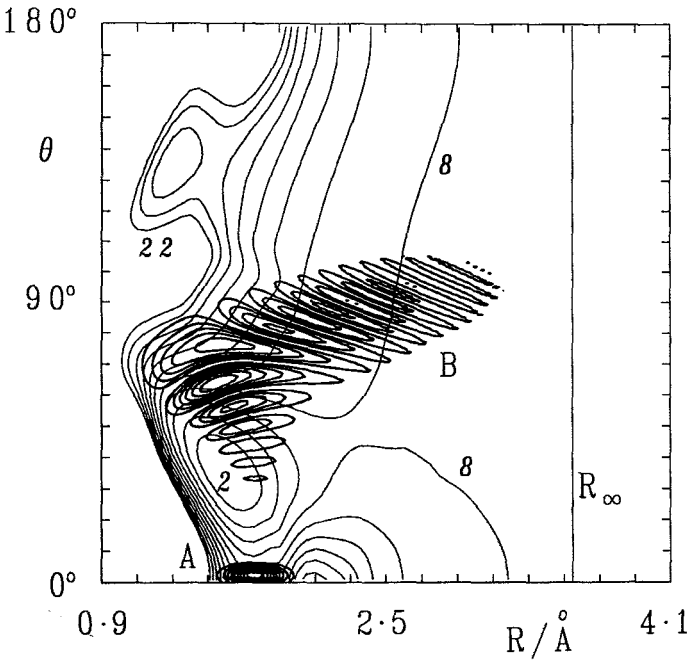

Figure 9. The time evolution of a wavepacket on the *ab initio* ground state potential energy surface (Bowman *et al.* 1986) of HCO. R and θ are Jacobi coordinates for H relative to CO. (*A*), the wavepacket at $t=0$; (*B*), the real component at $t=15{\cdot}9$ fs. The asymptotic analysis of the wavepacket to give CO rotational populations is carried out at $R=R_\infty$. The energy interval between potential contours is $2000\,\mathrm{cm}^{-1}$; three contours are labelled with the values of $V/(1000\,\mathrm{cm}^{-1})^{-1}$.

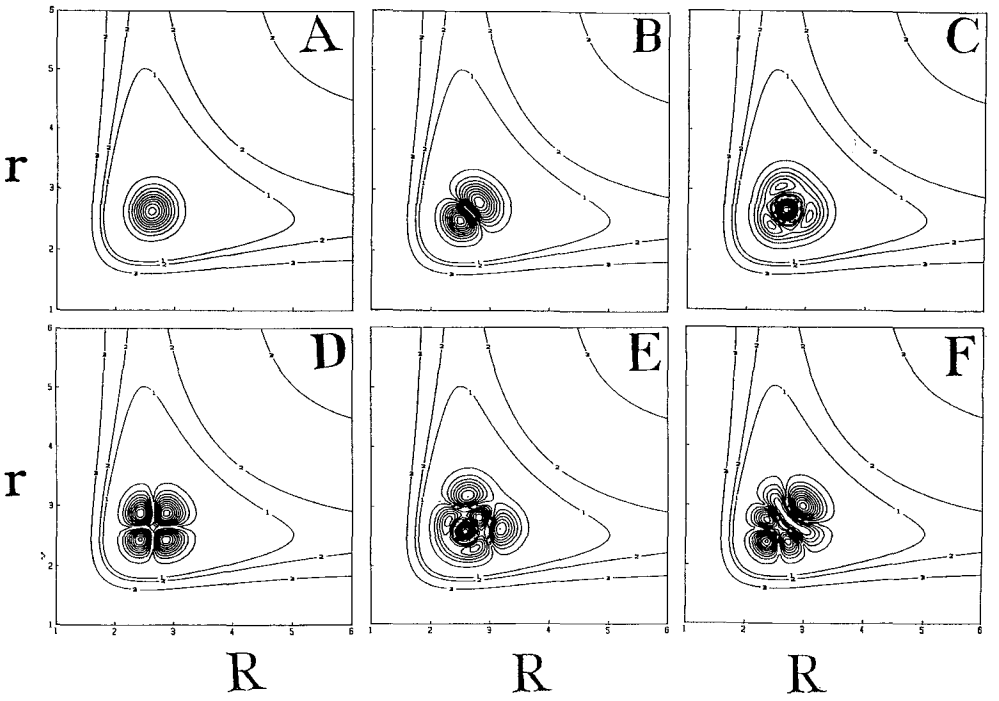

Figure 11. Vibrational wavefunctions of ground electronic state of H_2S using the symmetrized local mode model (see Dixon *et al.* (1990)). The correspondence between the panel labels and local mode vibrational quantum numbers is (A) 00, (B) 10^+, (C) 11, (D) 20^+, (E) 21^+, (F) 22 (reproduced with permission from *J. chem. Phys.*, 1990, **93**, 6520).

the S atom as being infinitely heavy in comparison with the hydrogen atoms. These bound vibrational state wavefunctions are used in equation (60) to compute the 'Raman amplitudes' $f(v_1)$, which are needed in equation (59) to calculate the emission spectrum. From these two equations we can see yet again that a *single* computation of the time dependent wavepacket dynamics will yield all the information needed to compute the emission spectrum for all wavelengths of the incident radiation (v_1). Figure 12 shows a comparison of the experimental (Person *et al.* 1989) and calculated emission line strengths where we have amalgamated strongly overlapping lines. The agreement between the two seems excellent. However recent calculations have shown that the model is not able to reproduce the more detailed emission spectral information obtained by Brudzynski *et al.* (1990), and that further refinements are still required.

5. Theory of reactive scattering processes

The first time dependent quantum dynamical study of reactive scattering was performed by McCullough and Wyatt (1971). More recently the method has been used by Askar and Cakmak (1979), Kulander (1978), Kosloff and Kosloff (1983b), Leforestier (1984), Zhang and Kouri (1986) and most notably by Neuhauser and Baer (1989a, b c), Neuhauser *et al.* (1990, 1991). The recent successes of Neuhauser *et al.* in applying time dependent quantum dynamical techniques to reactive scattering processes has been based on using a grid representation of the wavefunction within a restricted inner 'strong interaction' region and switching to a basis set expansion in a set of rotational-vibrational functions in an 'outer' region where the interaction potential

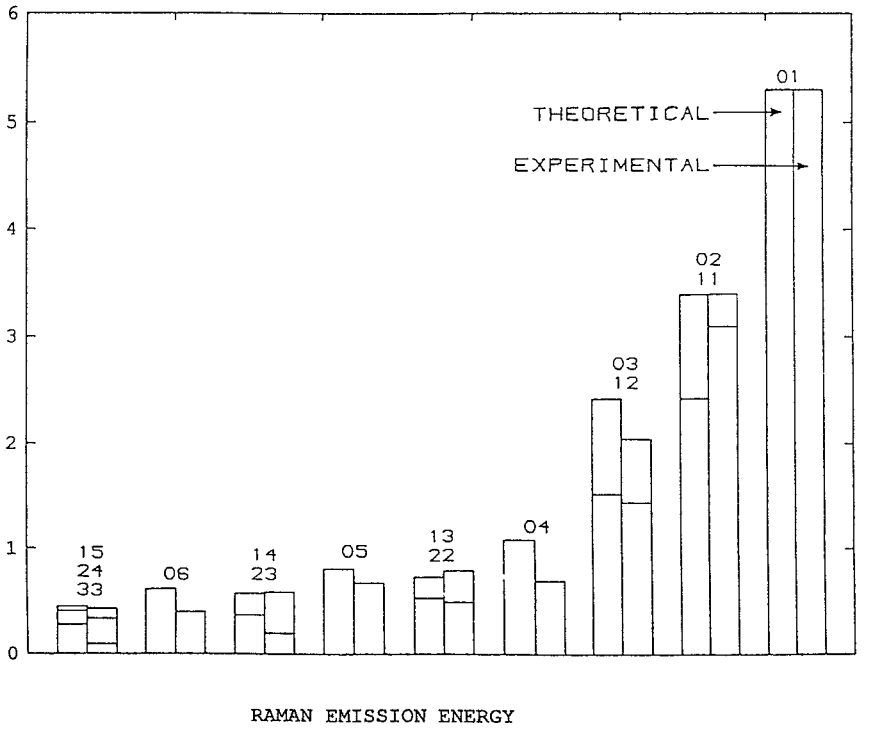

Figure 12. Comparison of calculated and experimental emission spectrum of H_2S during dissociation following absorption of an initial photon of 51 733 cm^{-1}. Strongly overlapping lines have been combined.

is weaker (Metiu 1987, Neuhauser *et al.* 1990). The joining up of the inner and outer regions leads to a set of coupled equations (Neuhauser and Baer 1989b, c), while the analysis of the product quantum state distribution requires a change of coordinates or grids as well as the use of projection operators and of a complex absorbing potential (Judson *et al.* 1991). Computation of the state-to-state reactive cross-sections requires the evaluation of the time independent scattering wavefunctions by performing a time to energy Fourier transform (Neuhauser *et al.* 1990).

The same methods as outlined above for photodissociation processes may be applied to the computation of reactive scattering cross sections. This approach is more straightforward than that of Neuhauser *et al.* It retains the simplicity of theory and transparency of interpretation which is a hallmark of grid based time dependent quantum dynamical methods (Marston *et al.* 1991). It should also permit a simpler way of utilising the great advantage of such methods by automatically yielding the reactive scattering cross-sections over a large range of energies. The first step in such a computation is to define an initial wavepacket. This is generally taken to be a Gaussian in the reactant scattering coordinate multiplied by a bound vibration–rotation state of the reactant fragments. This stationary Gaussian function must be multiplied by a phase factor of the form $\exp[-ik(R-R^0)]$ to give the initial wavepacket a relative kinetic energy. For the collinear $F+H_2(v)\rightarrow HF(v')+H$ reaction the initial wavepacket prepared in this way takes the form:

$$\Phi(R_{F-H_2}, R_{H-H}, t=0)=\exp[-ik(R_{F-H_2}-R^0_{F-H_2})]\exp[-\alpha(R_{F-H_2}-R^0_{F-H_2})^2]\,\phi_v(R_{H-H}). \tag{61}$$

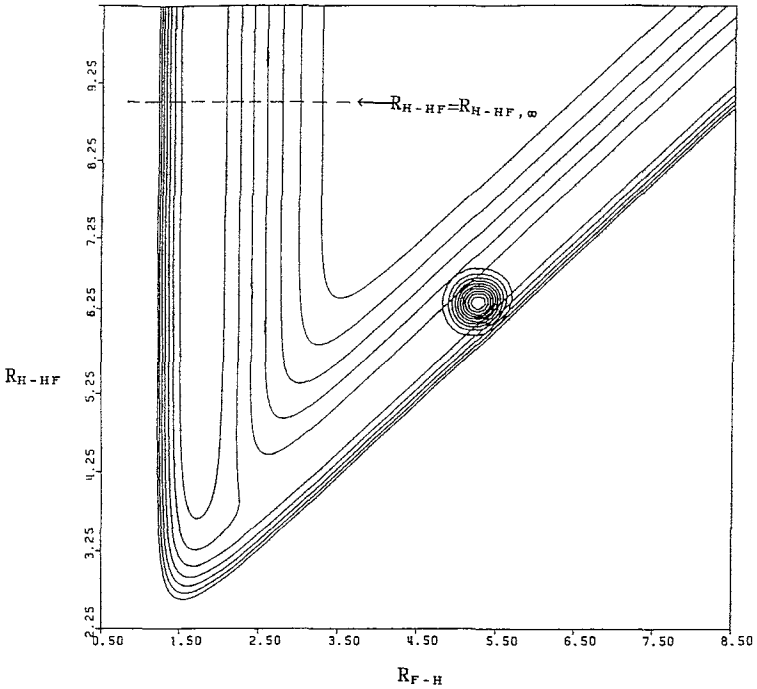

Figure 13. Contour plot of the absolute value of the initial wavepacket ($t=0$) for the $F+H_2(v)\rightarrow HF(v')+H$ reaction superimposed on a contour map of the potential energy surface. Also shown is the analysis line in the HF + H exit valley (i.e. $R_{H-HF}=R_{H-HF,\infty}$) along which the wavepacket is analysed at each time step (reproduced with permission from *Theor. chim. Acta*, 1991, **79**, 313).

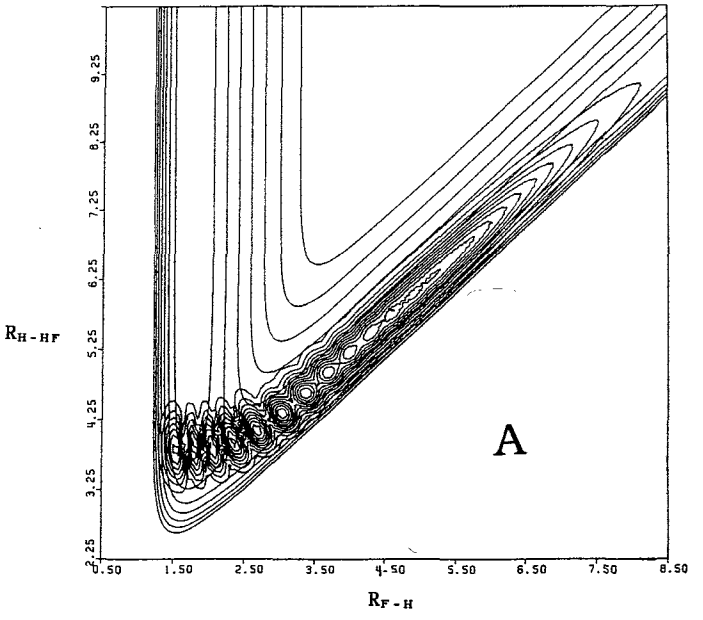

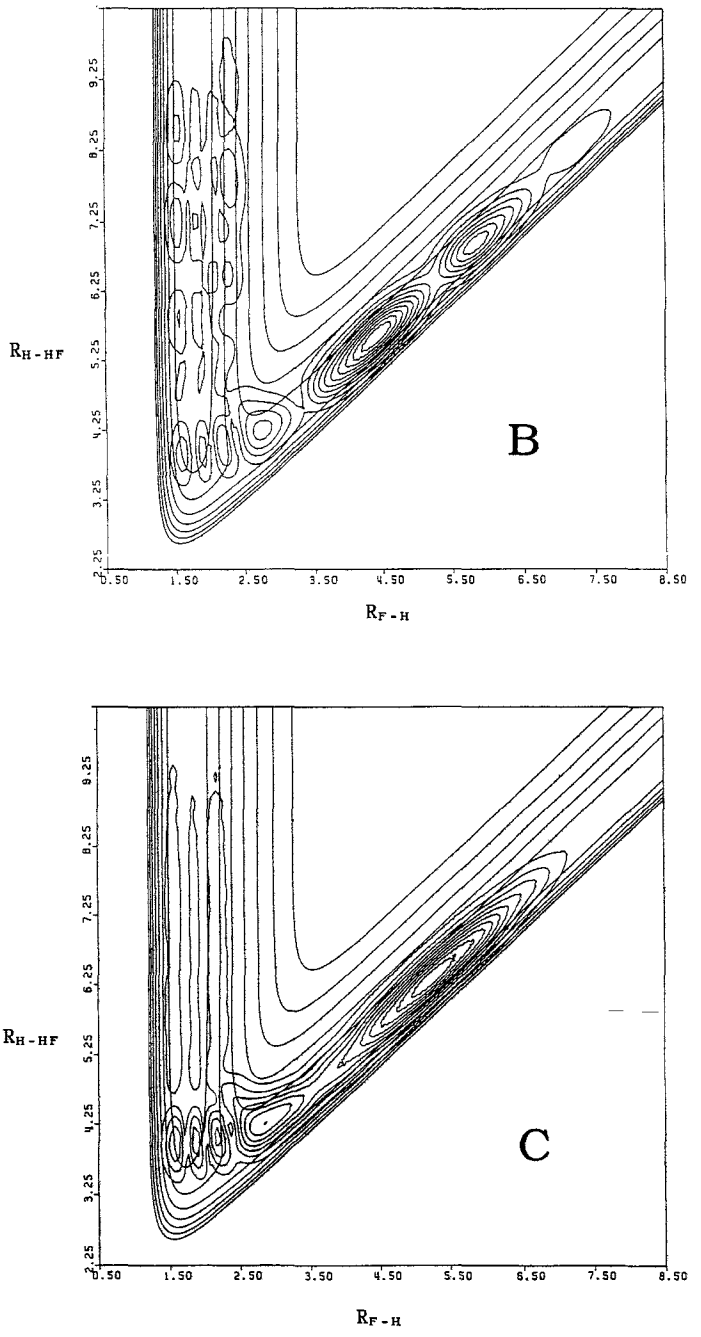

Figure 14. Time development of initially prepared wavepacket representing a reactive collision of the $F+H_2 \rightarrow HF(v)+H$ system in a model collinear collision process. (*A*) at 14·5 fs, (*B*) at 58·0 fs, (*C*) at 218·0 fs (reproduced with permission from *Theor. chim. Acta*, 1991, **79**, 313).

The 'width' parameter of the wavepacket, α, is chosen so as to obtain the desired spread of energy while the momentum, k, determines the mean relative kinetic energy of the collision partners. Figure 13 shows an initial wavepacket superimposed on a contour diagram of the potential energy surface for the collinear $F+H_2(v)\rightarrow HF(v')+H$ reaction. The diagram shows the 'analysis line'. Just as in the case of photodissociation processes a cut is taken through the wavepacket at each time step and this slice of the wavepacket is then expanded in terms of the product quantum states (see equations (55) and (56)). In this way we obtain a set of time dependent coefficients;

$$C_{v'}(R_{H-HF,\infty};t)=\int_0^\infty \phi_{v'}(R_{H-F})\Phi(R_{H-HF,\infty};R_{H-F};t)\,dR_{H-F}, \tag{62}$$

and the Fourier transform of these coefficients yields the corresponding energy dependent coefficients (see equation (57));

$$A_{v'}(R_{H-HF,\infty};E)=\frac{1}{2\pi}\int_{t=0}^{\infty}\exp(iEt/\hbar)\,C_{v'}(R_{H-HF,\infty};t)\,dt. \tag{63}$$

In order to compute the reactive scattering cross-section we need to know the amplitude of the initially prepared wavepacket which corresponds to a particular kinetic energy. This information is provided by the Fourier transform of the Gaussian wavepacket in the reactant scattering coordinates;

$$f(k_v)\phi_v(R_{H-H})=\frac{1}{2\pi}\int_{R=0}^{\infty}\exp(-ik_vR_{F-H_2})\,\Phi(R_{F-H_2},R_{H-H},t=0)\,dR_{F-H_2}. \tag{64}$$

A knowledge of the amplitude $f(k_v)$ (equation (64)) and of the energy dependent coefficients A_v (equation (63)) then enable us to compute the squares of the reactive scattering S matrix elements, and from them the reaction probabilities (for a collinear system) or the state-to-state reactive cross-sections for a fully three dimensional calculation;

$$P_{v,v'}=|S_{v'v}|^2=\frac{h^2}{4\pi^2\mu'^2}k_{v'}k_v\left|\frac{A_{v'}(R'_\infty,E)}{f(|k_v|)}\right|^2. \tag{65}$$

Figure 14 shows the time development of the initial wavepacket (figure 13) for the collinear $F+H_2(v)\rightarrow HF(v')+H$ reaction. We see that a clear nodal structure develops with time and is maintained for a considerable time. This structure corresponds to the 'reactive resonance' which has been well documented for this system. The time dependent coefficients $C_{v'}(R_{H-HF,\infty};t)$, equation (62), are shown in figure 15 for the two principal product HF quantum states. The coefficients should die off to zero with increasing time. They did not do so in the preliminary calculations performed so far and an artificial damping function has been applied to them the force this correct physical behaviour (Marston *et al.* 1991). We believe that the reason for this shortcoming lies in the manner in which the wavepacket was damped our near the edge of the grid. A thorough study of the optimal complex damping potentials to be used for this purpose has just been completed and will be published in the near future (Vibók and Balint-

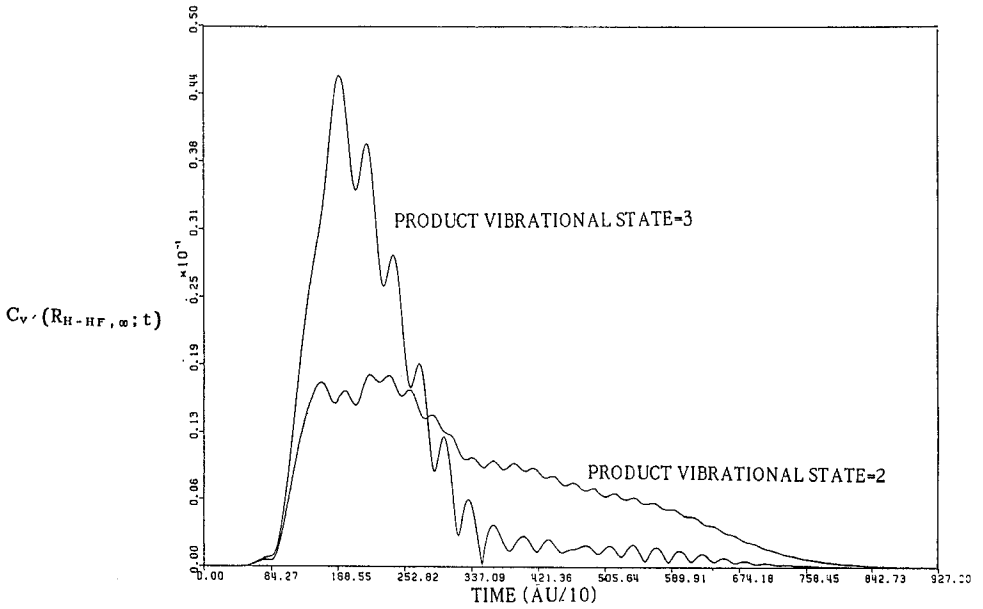

Figure 15. The absolute values of the time dependent coefficients $C_{v'}(R_{H-HF,\infty};t)$ for the $v'=2$ and $v'=3$ HF product vibrational quantum states resulting from the asymptotic analysis of the wavepacket for the collinear $F+H_2 \rightarrow HF(v)+H$ reaction. The long time tail of the coefficients has been multiplied by an exponential damping factor (see Marston *et al.* (1991)), (reproduced with permission from *Theor. chim. Acta*, 1991, **79**, 313).

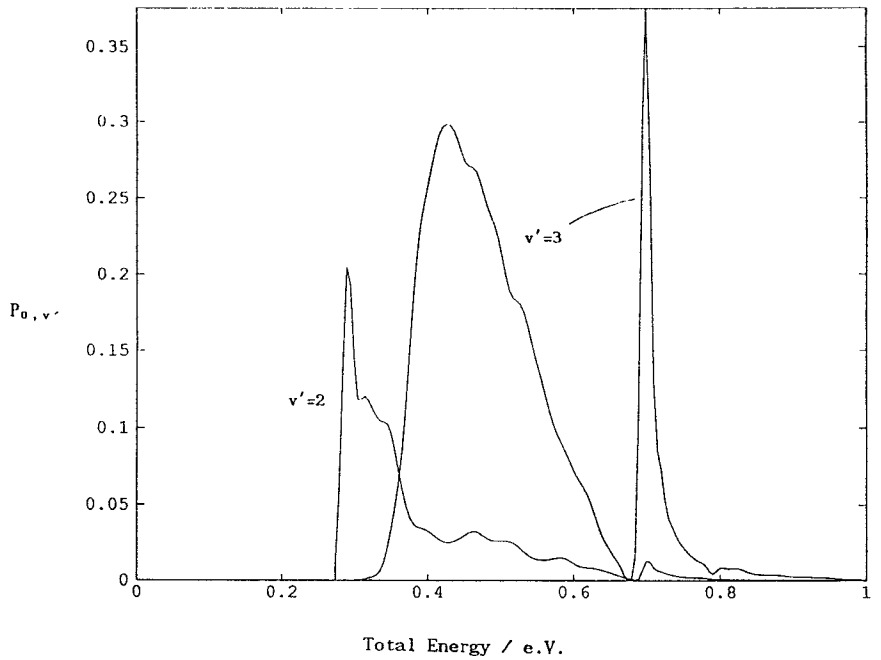

Figure 16. The probabilities of producing final HF vibrational quantum states $v'=2$ and $v'=3$ in the collinear reaction $F+H_2 \rightarrow HF(v)+H$ as a function of energy (see equation (64)) as obtained from the damped coefficients of figure 15, (reproduced with permission from *Theor. chim. Acta*, 1991, **79**, 313).

Kurti 1992). The results iof this study will enable us and others to choose optimised complex absorbing potentials for any desired physical situation.

Figure 16 (Marston *et al.* 1991) shows the reaction probabilities (equation (65)) for the two main product vibrational states as a function of energy. The resonance features are clearly visible and are all accurately predicted (see Schatz *et al.* (1975)). Some small oscillations in the energy dependence of the reaction probabilities arise from the artificial manner in which the time dependent coefficients have been damped for long times. The great advantage of the time dependent techniques is again illustrated through the fact that a single computation of the dynamics produces information on the reaction probabilities at all energies.

6. Summary

In the above a somewhat selective overview has been given of the current state of the theory of grid based methods as used for the computation of bound molecular vibrational wavefunctions and for molecular photodissociation and reactive scattering process. The main omission has been the lack of mention of the extensive use of the discrete variable representation (DVR) approach of Light and coworkers (Light *et al.* 1985, Light and Bacic 1987, Bacic, Watt and Light 1988). The grids generated by the DVR approach are not, in general (see however Whitnell and Light (1989)), regular and cannot be used in conjunction with Fourier transform techniques. The Fourier grid Hamiltonian method (Marston and Balint-Kurti 1989, Balint-Kurti *et al.* 1991), which is described in Section 2, provides an extremely simple way of computing bound state wavefunctions, while not explicitly involving any basis functions or potential energy matrix elements. It is furthermore ideally suited for use in conjunction with the regular grids used in the Fourier transform based methods which arise in time dependent quantum dynamics.

Most methods for solving the time dependent Schrödinger equation involve the use of grid methods, and since the work of Kosloff (1988) utilize the great efficiency of the discrete fast Fourier transform technique. They differ from time independent methods in that they are 'initial value' methods. That is we start from a known quantum state of either the initial electronically excited molecule (photodissociation) or of the reactants (reactive scattering) and the solution of the time dependent Schrödinger equation yields all possible outcomes of interest arising from this starting point. The logistics of including many highly excited initial quantum states, in which we have no real interest, for the sake of achieving numerical convergence is absent in this approach. Also the methods, as we have been applying them, automatically yield the cross-sections of interest over a very wide energy range from a single computation of the wavepacket dynamics. Illustrations of these advantages of time dependent quantum dynamics have been give in the equations (equations (53–60, 62, 63 and 65)) and in figures 7, 8, 12, 15 and 16. Methods such as those described here rely for their application on the rapidly growing power of new computer technology and as this continues to develop they will gain in popularity.

Acknowledgments

We thank A. Vibok for useful discussions and C. Li for assistance with the derivation of the analytic forms embodied in equation (52). We thank the SERC for their support through a research grant, for the provision of computational facilities on the Rutherford Laboratory Computer, and for providing funds for the purchase of a Meiko parallel computer on which our computations are currently being performed.

References

ASKAR, A., and CAKMAK, A. S., 1979, *J. chem. Phys.*, **68,** 2749.

BACIC, Z., WATT, D., and LIGHT, J. C., 1988, *J. chem. Phys.*, **89,** 947.

BALINT-KURTI, G. G., DIXON, R. N., and MARSTON, C. C., 1990, *J. chem. Soc. Faraday Transactions,* **86,** 1741.

BALINT-KURTI, G. G., and SHAPIRO, M., 1979, *J. chem. Phys.*, **71,** 1461; 1981, *Chem. Phys.*, **61,** 137.

BALINT-KURTI, G. G., WARD, C. L., and MARSTON, C. C., 1991, *Comput. phys. Commun.*, **67,** 285.

BOWMAN, J. M., BITTMAN, J. S., and HARDING, L. B., 1986, *J. chem. Phys.*, **85,** 911.

BRUDZYNSKI, R. J., SENSION, R. J. and HUDSON, B., 1990, *Chem. Phys. Lett.*, **165,** 487.

CHU, S.-I., 1990, *Chem. Phys. Lett.*, **167,** 155.

COLBERT, D. T., and MILLER, W. H., 1992, *J. chem. Phys.*, **96.** We thank W. H. Miller for pointing out to us that the summation in equation (50) could be performed analytically and for sending us a preprint of his paper.

DIRAC, P. A. M., 1958, *The Principles of Quantum Mechanics,* fourth Edition (Oxford: Clarendon Press).

DIXON, R. N., 1985, Molec. Phys., **54,** 333; 1992, *Chem. Phys. Lett.*, **190,** 430.

DIXON, R. N., MARSTON, C. C., and BALINT-KURTI, G. G., 1990, *J. chem. Phys.*, **93,** 6520.

FEIT, M. D., FLECK, J. A. Jr. and STEIGER, A., 1982, *J. comput. Phys.*, **47,** 412.

GRADSHTEYN, I. S., and RYZHIK, I. M., 1965, *Table of Integrals, Series and Products* (New York: Academic).

GRAY, S. K., and WOZNY, C. E., 1991, *J. chem. Phys.*, **94,** 2817.

HEATHER, R., and METIU, H., 1987, *J. chem. Phys.*, **86,** 5009.

HELLER, E. J., 1978, *J. chem. Phys.*, **68,** 2066; 1981, *Accts. Chem. Res.*, **14,** 368.

JUDSON, R. S., KOURI, D. J., NEUHAUSER, D., and BAER, M., 1990, *Phys. Rev.* A, **42,** 351.

KABLE, S. H., LOISON, J.-C., HOUSTON, P. L., and BURAK, I., 1990, *J. chem. Phys.*, **92,** 6332.

KOSLOFF, R., 1988, *J. phys. Chem.*, **92,** 2087, and references quoted therein.

KOSLOFF, D., and KOSLOFF, R., 1983a, *J. comput. Phys.*, **52,** 35; 1983b, *J. chem. Phys.*, **79,** 1823.

KOSLOFF, R., and KOSLOFF, D., 1986, *J. comput. Phys.*, **63,** 363.

KRISHNA, R. M. V., and COALSON, R. D., 1988, *Chem. Phys.*, **120,** 327.

KULANDER, K. C., 1978, *J. chem. Phys.*, **69,** 5064.

KULANDER, K. C., editor, 1991, Speical issue of *Comput. phys. Commun.*, **63.**

KULANDER, K. C., and HELLER, E. J., 1978, *J. chem. Phys.*, **69,** 2439.

LEE, S.-Y., and HELLER, E. J., 1979, *J. chem. Phys.*, **71,** 4777.

LEFORESTIER, C., 1984, *Chem. Phys.*, **87,** 241.

LEFORESTIER, C., BISSELING, R., CERJAN, C., FEIT, M. D., FRIESNER, R., GULDBERG, A., HAMMERICH, A., JOLICARD, G., KARRLEIN, W., MEYER, H.-D., LIPKIN, N., RONCERO, O., and KOSLOFF, R., 1991, *J. comput. Phys.*, **94,** 59.

LEHR, H., and CHATZIDIMITRIOU-DREISMANN, C. A., 1991, *Chem. Phys. Letts*, **186,** 511.

LIGHT, J. C., and BACIC, Z., J. C., 1987, *J. chem. Phys.*, **87,** 4008.

LIGHT, J. C., HAMILTON, I. P., and LILL, J. V., 1985, *J. chem. Phys.*, **82,** 1400.

MCCULLOUGH, E. A., and WYATT, R. E., 1971, *J. chem. Phys.*, **54,** 3578.

MARSTON, C. C., and BALINT-KURTI, G. G., 1989, *J. chem. Phys.*, **91,** 3571.

MARSTON, C. C., BALINT-KURTI, G. G., and DIXON, R. N., 1991, *Theor. chim. Acta*, **79,** 313.

NEUHAUSER, D., and BAER, M., 1989a, *J. chem. Phys.*, **90,** 4351; 1989b, *J. phys. Chem.*, **93,** 2872; 1989c, *J. chem. Phys.*, **91,** 4641.

NEUHAUSER, D., BAER, M., JUDSON, R. S., and KOURI, D. J., 1990, *Chem. Phys. Letts*, **169,** 372; 1991, *Comput. phys. Commun.*, **63,** 460.

NEUHAUSER, D., JUDSON, R. S., JAFFE, R. L., BAER, M., and KOURI, D. J., 1991, *Chem. Phys. Lett.*, **176,** 546.

PERSON, M. D., LAO, K. Q., ECKHOLM, B. J., and BUTLER, L. J., 1989, *J. chem. Phys.*, **91,** 812.

PRESS, W. H., FLANNERY, B. P., TEUKOLSKY, S. A., and VETTERLING, W. T., 1986, *Numerical Recipes* (Cambridge University Press).

SCHATZ, G. C., BOWMAN, J. M., and KUPPERMANN, A., 1975, *J. chem. Phys.*, **63,** 674.

SCHINKE, R., 1991, *Faraday Discussions Chem. Soc.*, **91,** 31.

TANG, S. L., ABRAMSON, E. H., and IMRE, D. G., 1991, *J. phys. Chem.*, **95,** 4969.

UNTCH, A., WEIDE, K., and SCHINKE, R., 1991a, *Chem. Phys. Lett.*, **180,** 265; 1991b, *J. chem. Phys.*, **95,** 6496.

VIBÓK, Á., and BALINT-KURTI, G. G., 1992a, *J. chem. Phys*, (in press); 1992b, (to be published).

WHITNELL, R. M., and LIGHT, J. C., 1989, *J. chem. Phys.*, **90,** 1774.
WILLIAMS, C. J., QIAN, J. W., and TANNOR, D. J., 1991, *J. chem. Phys.*, **95,** 1721.
XIE, X., SCHNIEDER, L., WALLMEIER, H., BOETTNER, R., WELGE, K. H., and ASHFOLD, M. N. R., 1990, *J. chem. Phys.*, **92,** 1608.
ZHANG, J. Z., HELLER, E. J., HUBER, D., and IMRE, D. G., 1991, *J. Phys. Chem.*, **95,** 6129.
ZHANG, Z. H., and KOURI, D. J., 1986, *Phys. Rev.* A, **34,** 2687.